Theor Chem Acc (2000) 103:445–450
DOI 10.1007/s002149900055

Theoretical
Chemistry Accounts

Regular article

Ab initio configuration interaction study on electronically excited 4-dimethylamino-4′-cyanostilbene

Yoshiaki Amatatsu

Faculty of Engineering and Resource Science, Akita University, Tegata Gakuen-cho, Akita 010-8502, Japan

Received: 16 December 1998 / Accepted: 19 March 1999 / Published online: 9 September 1999

Abstract. Ab initio configuration interaction calculations have been performed to examine the electronic structures of both *trans*-4-dimethylamino-4′-cyanostilbene (DCS) and four types of perpendicularly twisted DCSs, *trans*-DCS is predominantly excited into the S_1 state out of low-lying excited states. The S_1 state is an intramolecular charge-transfer (ICT) state in which the dipole moment is about twice as large as that in S_0. The excited DCS at the 4-dimethylanilino twisted conformation, which becomes S_1 in polar solvents, has a very much larger dipole moment than that in S_1 to *trans*-DCS. This means that the geometrical structure of the twisted ICT (TICT) is the 4-dimethylanilino twisted form, not the dimethylamino twisted one which is well know from the TICT structure of 4-dimethylaminobenzonitrile.

Key words: Ab initio configuration interaction calculation – 4-Dimethylamino-4′-cyanostilbene – Push–pull stilbene – Excited states – Intramolecular charge-transfer state

1 Introduction

4-Dimethylamino-4′-cyanostilbene (DCS), which has both electron donating and accepting groups, is a typical push–pull stilbene and is well known to be capable of photoinduced intramolecular charge transfer (CT) in polar solvents [1–18]. In spite of much effort to elucidate the electronic structure and dynamics of DCS in excited states, there is no widely accepted picture of them. The recent experimental findings are summarized as follows:

1. In polar solvents, there are two species which are characterized by red-shifted fluorescence [14–16, 18]. The first species, which is observed in the region of shorter wavelengths, is instantaneously formed during pulse excitation, then decays within a few picoseconds. The second one is formed as the first one decays. In other words, there is a precursor–successor relationship between them. The second species has a much longer lifetime of several hundred picoseconds and its emission is observed in the longer wavelength region. The emission wavelengths of the two species and the decay rate from the first species to the second one are dependent on the solvent polarity.

2. In nonpolar solvents, on the other hand, only one excited species is observed [15, 16, 18].

3. The cis–trans photoisomerization, which is followed by nonradiative relaxation into S_0 at the twisted conformation, is a competitive route against the formation reaction of the second species in the experimental findings 1. The isomerization route from *trans*-DCS to twisted DCS in S_1 has only a small energy barrier in the gas phase [13], while it is practically hindered in polar solvents [9, 11, 15, 16, 18].

In order to give a reasonable interpretation of the experimental findings and to establish a new picture of this reaction, we performed ab initio configuration interaction (CI) calculations and estimated the free energy in polar solvents by means of Onsager's reaction-field model. In order to justify the estimation, we also performed state-specific multiconfiguration self-consistent field (MCSCF) calculations combined with a polarizable continuum model. In the present paper, we focus on giving a reasonable interpretation of experimental findings 1 and 2 mentioned above based on ab initio results.

2 Method of calculations

The geometrical parameters of *trans*-DCS in S_0 were fully optimized at the restricted Hartree–Fock level with a Huzinaga–Dunning double-zeta basis set augmented by polarization functions on the N atoms ($\alpha_d = 0.80$) [19]. Then CI calculations were performed to characterize the electronically excited states as well as the ground state. Here polarization ($\alpha_d = 0.75$) and diffuse ($\alpha_p = 0.0438$) functions were added to the original basis set on the linkage ethylenic two carbon atoms in order to ensure the flexibility of orbitals derived from them, following the calculation for stilbene [20]. The configuration state functions (CSFs) taken into account in the CI calculations were those including up to triple excitations from the nine occupied π orbitals and the lone-pair orbitals on the N atoms to the lowest ten unoccupied π^* orbitals and low-lying diffuse un-

occupied ones. In order to calculate the free energies in polar solvents, we performed state-specific MCSCF calculations combined with a polarizable continuum model [21]. We used the GAMESS program [22] in the present ab initio calculation.

3 Results

First of all, we mention the optimized structure of *trans*-DCS in S_0. All optimized parameters are listed in Table 1. The numberings of atoms and the definition of the four torsional coordinates are shown in Fig. 1. The stilbene skeleton including the nitrile group is optimized to be planar, i.e. $\tau_2 = 0°$, $\tau_3 = 180°$, and $\tau_4 = 0°$. On the other hand, the structure of the dimethylamino part is calculated to be pyramidal, i.e., the wagging angle of the dimethylamino group against the plane spanned by the stilbene moiety is calculated to be 32.8° (τ_1 is −2.04°, not 0°), although in the case of optimization without polarization functions on the N atoms it is planar and so is unrealistic. Next we refer to the geometrical features of bond lengths. The bond length $R(C^1{=}C^2)$ is 1.3403 Å, which is similar to a normal C=C double bond. On the other hand, the bond lengths $R(C^1{-}C^3)$ and $R(C^2{-}C^9)$ are calculated to be 1.4733 and 1.4764 Å, respectively; so these linkage bonds of $C^1{-}C^3$ and $C^2{-}C^9$, which are connected with the ethylenic part and the phenyl groups, have normal C—C single-bond character and are not found to shrink due to π conjugation between the ethylenic part and the benzene rings. The bond lengths of the benzene skeletons, approximately 1.40 Å, take middle values between normal C—C single and C=C double bonds, which are similar to those of benzene. These features of bond lengths are also found in stilbene [20]. Furthermore, the $C^6{-}N^{15}$ length is 1.4017 Å, which is a value between normal C—N single and C=N double bonds. This means that the lone-pair electrons on the N atom of the dimethylamino group are resonant with the π electrons of the phenyl group connected with the dimethylamino one.

Next we mention the electronic structures of low-lying excited states of *trans*-DCS at the equilibrium geometry in S_0. The excitation energies, dipole moments, oscillator strengths, and the main CSFs of the first five excited states as well as of the ground state are listed in Table 2. It can be seen that the first excited-state manifold consists of S_1, S_2, and S_3 because the energy gap between S_3 and S_4 is large. The most characteristic point about the first excited-state manifold is that the dipole moment in S_1 (14.575 D) is about twice as large as that in S_0 (7.243 D). This can be explained by the character of the molecular orbitals (MOs) relating to the main CSF. The S_1 state is mainly described by the single excitation from the highest occupied MO (HOMO) to the lowest

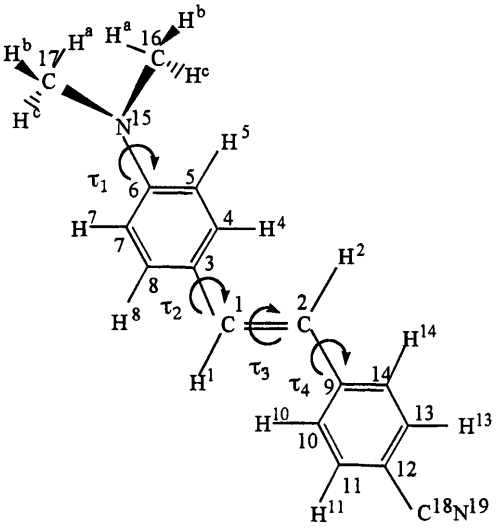

Fig. 1. Numberings of atoms of 4-dimethylamino-4′-cyanostilbene (*DCS*). The torsional degrees of freedom, τ_2, τ_3, and τ_4 are the dihedral angles $\angle C^4C^3C^1C^2$, $\angle C^9C^2C^1C^3$, and $\angle C^{10}C^9C^2C^1$, respectively. τ_1 is defined by the dihedral angle between two planes of which the normal vectors are $\{\mathbf{r}(C^6C^5) \times \mathbf{r}(C^6N^{15})\} \times \mathbf{r}(C^6N^{15})$ and $\{\mathbf{r}(N^{15}C^{16}) \times \mathbf{r}(N^{15}C^{17})\} \times \mathbf{r}(C^6N^{15})$. τ_1 at the optimized geometry of *trans*-DCS in S_0 is calculated to be −2.04° (not 0°)

Table 1. Optimized geometrical parameters of *trans*-4-dimethylamino-4′-cyanostilbene (*DCS*) in S_0

Bond lengths (Å)			
$R(C^1{-}C^2)$	1.3403	$R(C^1{-}H^1)$	1.0744
$R(C^1{-}C^3)$	1.4733	$R(C^2{-}H^2)$	1.0735
$R(C^3{-}C^4)$	1.4022	$R(C^4{-}H^4)$	1.0712
$R(C^4{-}C^5)$	1.3858	$R(C^5{-}H^5)$	1.0677
$R(C^5{-}C^6)$	1.4123	$R(C^7{-}H^7)$	1.0676
$R(C^6{-}C^7)$	1.4073	$R(C^8{-}H^8)$	1.0733
$R(C^7{-}C^8)$	1.3901		
$R(C^2{-}C^9)$	1.4764	$R(C^{10}{-}H^{10})$	1.0697
$R(C^9{-}C^{10})$	1.4059	$R(C^{11}{-}H^{11})$	1.0709
$R(C^{10}{-}C^{11})$	1.3867	$R(C^{13}{-}H^{13})$	1.0707
$R(C^{11}{-}C^{12})$	1.3998	$R(C^{14}{-}H^{14})$	1.0717
$R(C^{12}{-}C^{13})$	1.3961	$R(C^{16}{-}H^a)$	1.0790
$R(C^{13}{-}C^{14})$	1.3896	$R(C^{16}{-}H^b)$	1.0883
$R(C^6{-}N^{15})$	1.4017	$R(C^{16}{-}H^c)$	1.0801
$R(N^{15}{-}C^{16})$	1.4618	$R(C^{17}{-}H^a)$	1.0790
$R(N^{15}{-}C^{17})$	1.4608	$R(C^{17}{-}H^b)$	1.0885
$R(C^{12}{-}C^{18})$	1.4441	$R(C^{17}{-}H^c)$	1.0802
$R(C^{18}{-}N^{19})$	1.1405		
Bond angles (degrees)			
$\alpha(\angle C^3C^1C^2)$	127.25	$\alpha(\angle H^1C^1C^2)$	118.92
$\alpha(\angle C^4C^3C^1)$	124.13	$\alpha(\angle H^2C^2C^1)$	119.30
$\alpha(\angle C^5C^4C^3)$	121.84	$\alpha(\angle H^4C^4C^3)$	120.26
$\alpha(\angle C^6C^5C^4)$	121.48	$\alpha(\angle H^5C^5C^4)$	118.05
$\alpha(\angle C^7C^6C^5)$	116.73	$\alpha(\angle H^7C^7C^6)$	120.81
$\alpha(\angle C^8C^7C^6)$	121.06	$\alpha(\angle H^8C^8C^7)$	118.35
$\alpha(\angle C^9C^2C^1)$	126.54		
$\alpha(\angle C^{10}C^9C^2)$	123.69	$\alpha(\angle H^{10}C^{10}C^9)$	120.40
$\alpha(\angle C^{11}C^{10}C^9)$	121.05	$\alpha(\angle H^{11}C^{11}C^{10})$	119.98
$\alpha(\angle C^{12}C^{11}C^{10})$	120.35	$\alpha(\angle H^{13}C^{13}C^{12})$	119.92
$\alpha(\angle C^{13}C^{12}C^{11})$	119.36	$\alpha(\angle H^{14}C^{14}C^{13})$	119.15
$\alpha(\angle C^{14}C^{13}C^{12})$	119.96		
$\alpha(\angle N^{15}C^6C^5)$	121.41	$\alpha(\angle H^aC^{16}N^{15})$	108.87
$\alpha(\angle C^{16}N^{15}C^6)$	117.08	$\alpha(\angle H^bC^{16}N^{15})$	112.77
$\alpha(\angle C^{17}N^{15}C^6)$	117.03	$\alpha(\angle H^cC^{16}N^{15})$	110.82
$\alpha(\angle C^{13}C^{12}C^{11})$	120.26	$\alpha(\angle H^aC^{17}N^{15})$	108.89
$\alpha(\angle N^{19}C^{18}C^{12})$	180.0	$\alpha(\angle H^bC^{17}N^{15})$	112.84
		$\alpha(\angle H^cC^{17}N^{15})$	110.68
Dihedral angles (degrees)			
$\tau(\angle C^{16}N^{15}C^6C^5)$	−21.30	$\phi(\angle H^aC^{16}N^{15}C^6)$	−177.52
$\tau(\angle C^{17}N^{15}C^6C^7)$	17.19	$\phi(\angle H^aC^{16}N^{15}C^6)$	−57.04
		$\phi(\angle H^aC^{16}N^{15}C^6)$	65.01
$\tau(\angle C^4C^3C^1C^2)$	0.0	$\phi(\angle H^aC^{17}N^{15}C^6)$	179.01
$\tau(\angle C^9C^2C^1C^3)$	180.0	$\phi(\angle H^aC^{17}N^{15}C^6)$	58.46
$\tau(\angle C^{10}C^9C^2C^1)$	0.0	$\phi(\angle H^aC^{17}N^{15}C^6)$	−63.52

Table 2. Excitation energies, dipole moments, oscillator strengths, and the main configuration state functions (*CSFs*) of *trans*-DCS at the equilibrium structure in S_0

	Excitation energy (eV)	Dipole moment (D)	Oscillator strength	Main CSFs[a,b]
S_0	0.0	7.243		0.938(closed shell)
S_1	5.030	14.575	1.306	+0.835(1-1′) + 0.226(1-2′) + 0.157(1-3′) − 0.154(2-3′) + 0.125(2-1′) + 0.117(4′-1)
S_2	5.372	8.779	0.119	+0.564(4-1′) + 0.375(2-2′) + 0.372(1-2′) − 0.272(1-3′) − 0.204(1-1′) − 0.150(2-3′) + 0.135(4-5′) + 0.125(5-2′)
S_3	5.465	8.645	0.236	+0.474(1-3′) − 0.378(1-4′) − 0.340(3-1′) + 0.328(1-2′) − 0.249(1-1′) + 0.220(3-5′) − 0.158(3-3′) + 0.153(1-5′) − 0.147(3-4′) + 0.127(2-4′) − 0.124(1-6′)
S_4	6.498	12.161	1.59×10^{-4}	+0.910(1-*R*) + 0.137(2-*R*) + 0.121(5-*R*)
S_5	6.544	9.944	0.056	+0.771(2-1′) − 0.243(1^2-$1'^2$) − 0.126(4-2′) − 0.125(4-1′) − 0.120(2-5′) + 0.116(5-1′) + 0.107(5-5′) − 0.106(2,1-1′,5′) − 0.104(2,1-$1'^2$)

[a] The CSFs with absolute values of configuration interaction coefficients greater than 0.1 are listed. The highest five occupied π orbitals and the lowest six unoccupied π^* ones in the order of energy are designated by 5,4,3,2,1(HOMO),1′(LUMO),2′,3′,4′,5′,6′, respectively. 1-1′ in parentheses, for instance, indicates the CSF of single excitation from orbital 1 to 1′

[b] *R* denotes the lowest diffuse orbital

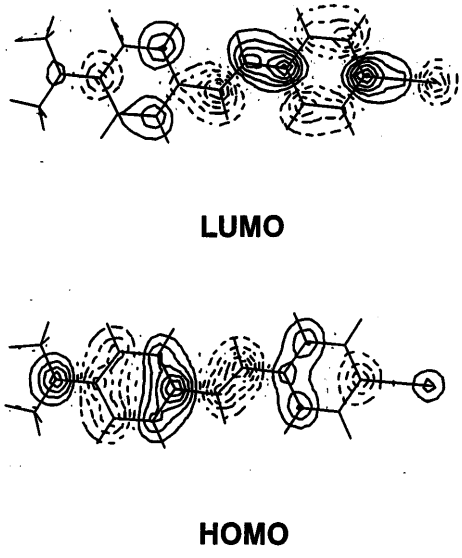

Fig. 2. Highest occupied molecular orbital (*HOMO*) and lowest unoccupied molecular orbital (*LUMO*) of *trans*-DCS

unoccupied MO (LUMO). As seen in Fig. 2, the HOMO has a relatively high electron density in the region of the 4-dimethylanilino group (the dimethylamino group and the benzene moiety connected with it) as well as in the linkage ethylenic part, while the LUMO is able to accept the electron in the region of the 4-cyanostyryl group; therefore, S_1 is expected to be an internal CT (ICT) state in which the electron is transferred from the 4-dimethylanilino group to the 4-cyanostyryl one. This is in agreement with the deduction that S_1 at the Franck–Condon (FC) region is already an admixture of CT and locally π π^* excited character based on experimental findings [11, 14–16, 18]. Another notable point seen in Table 2 is that *trans*-DCS is preferentially excited into S_1 out of the first excited-state manifold. This is due to the fact that both the matrix element of the transition dipole by HOMO–LUMO excitation itself (9.53 D) and the weight of the CSF derived from HOMO–LUMO single excitation (0.835) are large. The two results, i.e. the transition into S_1 is dominant and the dipole moment in S_1 is twice as large as that in S_0 at the FC region, imply that the emission at the FC region is red-shifted in polar solvents, which is in agreement with experimental findings [14–16, 18].

Next we mention the electronic structures of the four types of perpendicularly twisted DCSs and discuss the excited states of these DCSs in polar solvents. The energy differences and dipole moments of the four (τ_1–τ_4) twisted conformations as well as those at the equilibrium structure are listed in Table 3. The energy differences in the polar solvent water estimated by means of Onsager's reaction-field model are also included. The striking point is that the dipole moment in S_4 of the τ_2-twisted conformation (29.569 D) is about twice as large as that in S_1 at the FC region (14.575 D) and so S_4 in the gas phase becomes a global minimum in S_1 in polar solvents. On the other hand, the dipole moment in S_0 at the τ_2-twisted DCS conformation is not large and is similar to that at the FC region. This implies that the energy difference between S_0 and S_1 for τ_2-twisted DCS is smaller than that at the equilibrium geometry of the trans form. In other words, the emission from τ_2-twisted DCS is more red-shifted than that at the FC region in polar solvents. Here it is worthwhile explaining why the dipole moment in S_4 of τ_2-twisted DCS is enormous. The main CSF is still HOMO–LUMO single excitation (0.841 CI coefficient). As shown in Fig. 3, the electron in the HOMO lies exclusively in the region of the 4-dimethylanilino group, while the LUMO has the character to accept the electron only in the region of the remaining moiety, i.e., the 4-cyanostyryl group; therefore the HOMO–LUMO single excitation causes the electron to be perfectly transferred from the 4-dimethylanilino group to the

4-cyanostyryl one. As mentioned previously, the electron transfer derived from the HOMO–LUMO single excitation is partly seen even at the FC region just after excitation from S_0 and S_1. As τ_2 increases, however, the electron transfer from the 4-dimethylanilino group to the 4-cyanostyryl one is gradually promoted and it is completed at $\tau_2 = 90°$. This electron-transfer process can also be rationalized in terms of the change in charge populations. The Mulliken charges on each atom for the three states relating to this process, i.e., S_0 and S_1 at the FC region of *trans*-DCS, and S_4 at the τ_2-twisted DCS conformation, are listed in Table 4. By the electronic excitation from S_0 to S_1 at *trans*-DCS, the charge in the region of the 4-dimethylanilino group moves to the 4-cyanostyryl one by 0.226*e*. Furthermore, at the perpendicularly τ_2-twisted conformation, the charge separation between the two groups is accomplished. As also shown in Table 3, the excited states of τ_1- or τ_3-twisted DCS in polar solvents cannot be expected to be stabilized so much that emissions at these twisted conformations are not observed. As to the τ_4-twisted form, the dipole moments of the S_4 and S_5 states in the gas phase also take large values and so are stabilized into S_1 and S_2 in polar solvents, respectively; however, these are still above S_1 at the FC region as well as the global minimum in S_1, i.e., S_1 at the τ_2-twisted DCS conformation. Therefore, the second type of emission is unlikely to be assigned to the emission from S_1 at τ_4-twisted DCS.

The above discussion on the electronic structures of DCS in polar solvents is based on Onsager's reaction-field model. In this model, a solute dipole is placed within a cavity of a dielectric continuum producing a reaction field; so only the interaction of the solute dipole with the solvent is taken into account and the other terms, such as repulsion and dispersion, are completely ignored. In the process treated here, the changes in the dipole moments are enormous but the volume of the cavity containing the solute molecule can be assumed to be not changed so much by the torsional motion;

Table 3. Energy differences (eV) and dipole moments (D) at trans and twisted conformations of DCS

		Trans	τ_1 twisted	τ_2 twisted	τ_3 twisted	τ_4 twisted
S_0	ΔE_i^{gas} [a]	0.0	0.880	0.250	3.675	0.315
	ΔE_i^{solv} [b]	0.0	0.935	0.278	3.740	0.327
	$\lvert\mu_i\rvert$	7.243	5.914	6.617	5.636	6.975
S_1	ΔE_i^{gas}	5.030	6.290	5.715	4.866	5.831
	ΔE_i^{solv}	4.527	6.106	5.739	4.242	5.770
	$\lvert\mu_i\rvert$	14.575	10.532	6.696	15.832	8.478
S_2	ΔE_i^{gas}	5.372	6.799	6.016	7.486	5.997
	ΔE_i^{solv}	5.294	6.795	5.920	7.582	6.005
	$\lvert\mu_i\rvert$	8.779	7.316	9.107	4.678	7.065
S_3	ΔE_i^{gas}	5.465	6.955	6.417	7.588	6.342
	ΔE_i^{solv}	5.395	6.983	6.340	7.721	6.060
	$\lvert\mu_i\rvert$	8.645	6.588	8.785	3.195	11.934
S_4	ΔE_i^{gas}	6.498	7.763	6.723	7.728	6.858
	ΔE_i^{solv}	6.198	7.771	4.138	7.779	4.792
	$\lvert\mu_i\rvert$	12.161	7.054	29.569	6.015	26.632
S_5	ΔE_i^{gas}	6.544	7.916	7.182	7.740	7.320
	ΔE_i^{solv}	6.398	7.931	6.973	7.829	6.007
	$\lvert\mu_i\rvert$	9.944	6.918	10.961	4.922	21.682

[a] ΔE_i^{gas} is estimated using $\Delta E_i^{\text{gas}} = E_i^{\text{gas}} - E_0^{\text{gas}}$

[b] ΔE_i^{solv} is estimated using $E_i^{\text{solv}} = (E_i^{\text{gas}} - E_i^{\text{solv}}) - (E_0^{\text{gas}} - E_0^{\text{solv}})$. $E_i^{\text{solv}} = (\varepsilon - 1)/(2\varepsilon + 1) \times |\mu_i^2|/(4\pi\varepsilon_0\rho^3)$, where $\varepsilon = 78.5$ for water, and $\rho = 4.6$ Å for the radius of the cavity of DCS taken from Ref. [15]. It is assumed that ρ is constant for all conformations

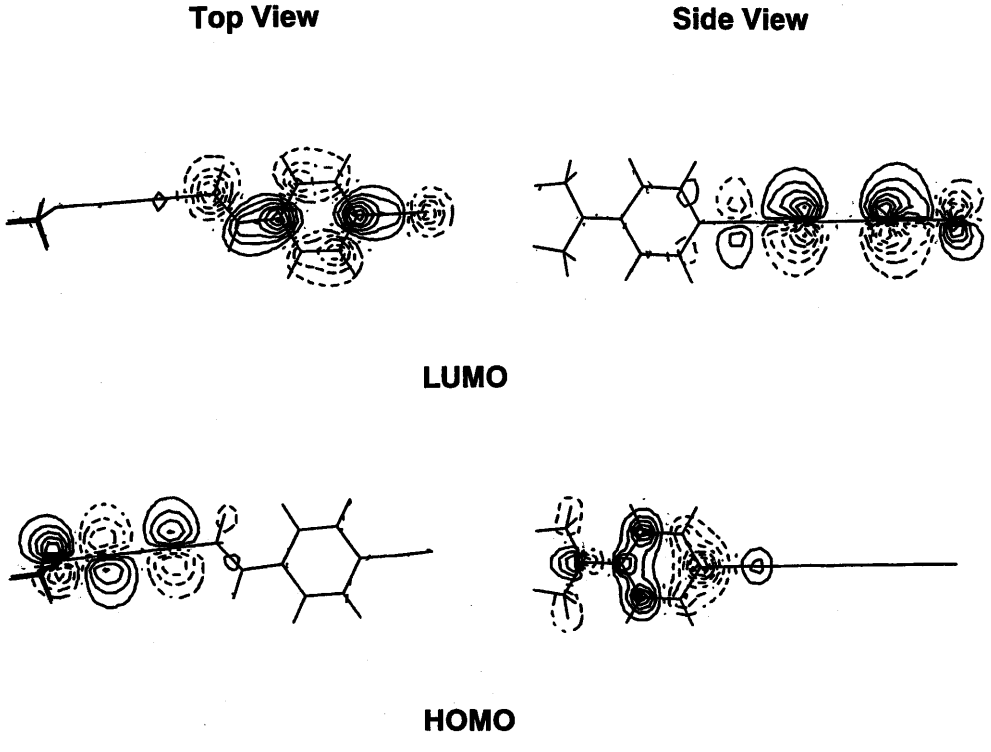

Fig. 3. HOMO and LUMO of τ_2-twisted DCS

Table 4. Mulliken charges of S_0 and S_1 at the *trans*-DCS conformation and S_4 at the τ_2-twisted DCS conformation

	Trans		τ_2 twisted
	S_0	S_1	S_4
C^1	−0.264	−0.332	−0.742
C^2	−0.276	−0.283	−0.307
C^3	0.477	0.561	0.588
C^4	−0.346	−0.391	−0.272
C^5	−0.320	−0.288	−0.224
C^6	0.471	0.494	0.564
C^7	−0.322	−0.337	−0.238
C^8	−0.377	−0.323	−0.247
C^9	0.473	0.443	0.403
C^{10}	−0.317	−0.384	−0.395
C^{11}	−0.305	−0.294	−0.317
C^{12}	0.234	0.208	0.139
C^{13}	−0.299	−0.355	−0.356
C^{14}	−0.352	−0.308	−0.355
N^{15}	−0.462	−0.384	−0.291
C^{16}	−0.385	−0.384	−0.391
C^{17}	−0.388	−0.387	−0.394
C^{18}	0.023	0.015	0.029
N^{19}	−0.225	−0.244	−0.292
H^{20}	0.172	0.172	0.207
H^{21}	0.176	0.176	0.200
H^{22}	0.176	0.176	0.188
H^{23}	0.196	0.196	0.193
H^{24}	0.199	0.199	0.195
H^{25}	0.182	0.182	0.190
H^{26}	0.188	0.188	0.194
H^{27}	0.215	0.215	0.218
H^{28}	0.216	0.216	0.217
H^{29}	0.196	0.196	0.201
H^{30}	0.170	0.169	0.172
H^{31}	0.169	0.175	0.188
H^{32}	0.183	0.183	0.187
H^{33}	0.170	0.170	0.173
H^{34}	0.168	0.175	0.186
H^{35}	0.184	0.185	0.188
4-Dimethylanilino	0.145	0.371	0.955
4-Cyanostyryl	−0.145	−0.371	−0.955

therefore, the electrostatic interaction strongly depends on the electronic structure and its geometrical conformation but the other terms are not expected to be affected by them. This implies that even a crude estimation of the free energy by means of Onsager's reaction-field model can give a good picture of this photochemical process. In order to justify the above assumption, we performed a more reliable calculation for the electronic structures in polar solvents, i.e., a MCSCF calculation combined with a polarizable continuum model, which includes not only electrostatic interaction but also the repulsive and dispersion terms. Since the three states in question can be well described by a closed-shell configuration for S_0 at the equilibrium geometry of *trans*-DCS (0.938 CI coefficient) and HOMO–LUMO single excitation for S_1 at the *trans* conformation and S_4 at the τ_2-twisted one (0.835 and 0.841, respectively), a state-specific two-configuration SCF calculation combined with a polarizable continuum model is suitable to estimate the free energies and to reduce computational labor. The free energies in water for these states are listed in Table 5. It can be seen that S_1 at the τ_2-twisted DCS conformation is more stabilized than that at the *trans*-DCS conformation in the polar solvent water. As already pointed out, the electrostatic interactions are strongly affected by both the geometrical and electronic structures of DCS, while the other terms are similar to one another. This means that the DCS behavior in polar solvents can be deduced by means of a simple Onsager reaction-field model.

Based on the present calculations, we give a reasonable interpretation of experimental findings 1 and 2 mentioned in the Introduction. The dipole moment of S_1 even at the FC region is already twice as large as that in S_0 and so S_1 is more stabilized than S_0 in polar solvents, therefore, the emission from S_1 at the FC region is red-shifted. Furthermore, by twisting the τ_2 coordinate, excited DCS is more stabilized in polar solvents which causes the direct change from *trans*-DCS into τ_2-twisted DCS in S_1. Once τ_2-twisted DCS in S_1 with a gigantic dipole moment is produced in polar solvents, this state is stabilized sufficiently to have a longer lifetime, while the corresponding S_0 state is not so stabilized; therefore the energy difference between them at the τ_2-twisted region becomes smaller than that at the FC region. These are explanations for why the lifetime of excited τ_2-twisted DCS is much longer and why this second type of emission is observed at longer wavelengths. In nonpolar solvents, on the other hand, the excited state with a gigantic dipole moment at the τ_2-twisted conformation cannot be stabilized and so the second type of emission is not observed.

Before terminating the discussion, we would like to point out that the twisted ICT (TICT) formation mechanism and the geometrical structure of DCS mentioned above are quite different from those of 4-dimethylaminobenzonitrile (DMABN), which has been studied more. According to theoretical approaches [23–25] DMABN at the FC region has locally $\pi\ \pi^*$ excited character is S_1, but CT character in S_2 at the FC region even in polar solvents. The transition intensity of S_0 to S_2 is much larger than that of S_0 to S_1. At the dimethylamino-twisted form, excited DMABN in polar solvents becomes S_1 due to a larger dipole moment. Therefore, following the first step that DMABN is preferentially excited into S_2 at the FC region, excited DMABN can have two kinds of relaxation route, i.e. one is fluorescence from S_1 at the FC region after internal conversion of S_2 into S_1, and the other is red-shifted fluorescence at the TICT produced through the

Table 5. Free energies and their components (eV) at 298 K

	Trans		τ_2 twisted
	S_0	S_1	S_1
Internal energy	−20730.709	−20725.120	−20724.605
Electrostatic interaction	−0.445	−0.881	−1.687
Cavitation energy	1.728	1.728	1.740
Dispersion energy	−1.105	−1.220	−1.233
Repulsion energy	0.460	0.480	0.486
Total free energy	−20730.071	−20725.013	−20725.299

torsional motion of the dimethylamino group. The difference in the TICT formation dynamics between DMABN and DCS originates from the character of the electronic structures. A detailed and comparative discussion will be published elsewhere.

4 Concluding remarks

In this paper, we reported both electronic and geometrical features of DCS deduced by means of ab initio calculations. For the optimized structure in S_0, the dimethylamino group has a pyramidal structure, but the remaining portion is planar. The 4-dimethylanilino group and the 4-benzonitrile one are connected with the ethylenic part through C—C bonds which have single-bond character. On the other hand, there is some π conjugation of the dimethylamino group with the phenyl one, which leads to a shortening of the corresponding C—N bond compared to a normal C—N single bond. For the excited states, *trans*-DCS has a large transition intensity from S_0 into S_1 out of low-lying excited states. S_1 is an ICT state in which the electron is transferred from the 4-dimethylanilino group to the 4-cyanostyryl one. This electron transfer can be accomplished by perpendicularly twisting the C—C bond connecting the 4-dimethylanilino group with the 4-cyanostyryl one; so the 4-dimethylanilino twisted form comes to have a much larger dipole moment, which is enough for excited DCS to become a global S_1 minimum in polar solvents while it is not stabilized in nonpolar solvents. In this study, we gave a qualitative but reasonable picture of the dynamics of the TICT formation. What we should do next is to give a quantitative and detailed picture of it. This is now in progress.

Acknowledgements. The numerical calculations were partly performed at the Computer Center of the Institute for Molecular Science. This work is financially supported by a Grant-in-Aid for Encouragement of Young Scientists (nos. 08740439 and 09740414) from the Ministry of Education, Science, Sport, and Culture.

References

1. Rettig W (1994) In Mattay J (ed): Topics in current chemistry, vol 169. Electron transfer I. Springer, Berlin Heidelberg New York, p. 243
2. Rettig W, Majeix W, Herter R, Létard JF, Lapouyade R (1993) Pure Appl Chem 65: 1699
3. Lippert E, Luder W, Moll F (1959) Spectrochim Acta 10: 858
4. Kawski A, Gryczynski I, Jung C, Heckner JH (1977) Z Naturforach A 32: 400
5. Kawski A, Kukieski J, Bauk P, Lenczewska M (1980) Z Naturforach A 35: 466
6. Gruen H, Gorner H (1983) Z Naturforach A 38: 928
7. Amiri AS (1986) Chem Phys Lett 125: 272
8. Gilabert E, Lapouyade R, Rullière C (1988) Chem Phys Lett 145: 262
9. Rettig W, Majenz J (1989) Chem Phys Lett 154: 335
10. Gilabert E, Lapouyade R, Rullière C (1991) Chem Phys Lett 185: 82
11. Lapouyade R, Czechka K, Majenz W, Rettig W, Gilabert E, Rullière C (1992) J Phys Chem 96: 9643
12. Rettig W, Gilabert E, Rullière C (1994) Chem Phys Lett 229: 127
13. Daum R, Hansson T, Norenberg R, Schwarzer D, Schroeder J (1995) Chem Phys Lett 246: 607
14. König NE, Köhne T, Schwarzer D, Vöhringer P, Schroeder J (1996) Chem Phys Lett 253: 69
15. Il'iochev YV, Kühnle W, Zacharinase KA (1996) Chem Phys 211: 441
16. Abraham E, Oberlé J, Jonusauskaa G, Lapouyade R, Rullière C (1997) Chem Phys 214: 409
17. Abraham E, Oberlé J, Jonusauskaa G, Lapouyade R, Minoshima K, Rullière C (1997) Chem Phy 219: 73
18. Abraham E, Oberlé J, Jonusauskaa G, Lapouyade R, Rullière C (1997) J Photochem Photobiol A 105: 101
19. (a) Huzinage S (1965) J Chem Phys 42: 1293; (b) Dunning TH Jr (1970) J Chem Phys 53: 2823
20. Amatatsu Y THEOCHEM (1999) 461–462: 311
21. Tomasi J, Persico M (1994) Chem Rev 94: 2027
22. Schmidt MW, Baldridge KK, Boats JA, Elbert ST, Gordon MS Jensen JH, Koseki S, Matsunaga N, Nguyen KA, Su SJ, Windus TI, Dupuis M, Montgomery JA Jr (1993) J Comput Chem 14: 1347
23. Kato S, Amatatsu Y (1990) J Chem Phys 92: 7241
24. Serrano-Andréa L, Merchán M, Root BO, Lindh R (1994) J Am Chem Soc 117: 3189
25. Hayashi S, Ando K, Kato S (1995) J Phys Chem 99: 955